

Electrical conductivity anomalies study

I.I. Rokityansky, A.V. Tereshyn, 2023

S.I. Subbotin Institute of Geophysics of the National Academy
of Sciences of Ukraine, Kyiv, Ukraine
Received 19 April 2023

Anomalous currents in a well-conducting body arise due to local electromagnetic induction inside the anomalous body, as well as due to conductive redistribution (and concentration) of currents induced in the host medium on a large territory equal to the external source size. The local induction generates the so-called anomaly of geomagnetic variations of the magnetic or inductive type. Its characteristic property is that the secondary anomalous field cannot be greater than the primary normal field of geomagnetic variations. However, in some places on the earth's surface, the normalized anomalous fields are greater than 1. Analytical solution of the EM induction problem for circular cylinder yields the physical explanation of two types of anomalous geomagnetic fields. The first term (proportional to the normal electric field E_0) describes the conductive anomaly type, the second term (proportional to the normal magnetic field B_0) describes the inductive anomaly type. The conductive type usually is much greater than the inductive one. The normalized anomalous field of the conductive type is not limited to 1 or any other value. It is proportional to two functions: $V(T)$ — the non-decreasing function of the period T ($0 \leq V \leq 1$, $V=1$ corresponds to DC) which describes the degree of filling of the conductor by anomalous currents (result of the skin effect inside the anomaly) and the normal impedance of inclosing cross-section — the decreasing function of the period. Product of these functions has a maximum at some period T_0 . The position T_0 is closely related to the total lengthwise conductance $G[S \times m]$ of the anomalous body, that is, the scale of the anomaly. On the period T_0 , the anomalous fields and the induction vector become real $\mathbf{C}=\mathbf{C}_u$ and the imaginary induction vector \mathbf{C}_v passes through zero changing sign. Thus, the spectral properties of the geomagnetic response functions were studied for two-dimensional anomalies with a generalization to three-dimensional conductors with varying cross-section. 18 crustal electrical conductivity anomalies were considered and their integral lengthwise conductance G was obtained. At all anomalies, the G values turn out to be in a relatively narrow range $G=(1-8) \cdot 10^8$ S·m; this has geophysical significance.

Key words: electrical properties, electromagnetic theory, geomagnetic induction, induction vector, magnetic variation profiling.

Introduction. Electrical conductivity $\sigma(r)$ is a physical parameter used to study solid Earth composition, structure, and physical state.

The deep Geoelectrics using natural electromagnetic (EM) fields of magnetosphere-ionosphere origin includes three methods.

GDS — geomagnetic deep sounding.

Source — spatial harmonics of the geomagnetic field, starting model — 1D concentric layered Earth.

MTS — magnetotelluric sounding. Source — vertically incident horizontally uniform EM field, starting model — 1D horizontally layered Earth. Both form the Tikhonov-Cagniard (T-C) model.

Citation: Rokityansky, I.I., & Tereshyn, A.V. (2023). Electrical conductivity anomalies study. *Geofizicheskiy Zhurnal*, 45(4), 116—127. <https://doi.org/10.24028/gj.v45i4.286288>.

Publisher Subbotin Institute of Geophysics of the NAS of Ukraine, 2023. This is an open access article under the CC BY-NC-SA license (<https://creativecommons.org/licenses/by-nc-sa/4.0/>).

MVP — magnetic variation profiling. Source — vertically incident horizontally uniform geomagnetic field, studied model — anomalies of electrical conductivity that are the strong deviations of the conductivity from the 1D horizontally layered Earth.

Of course, all three methods work with the same complex natural external EM field on the same complexly constructed Earth. The above field sources and earth models show those approximations for which basic mathematical models of each method have been created. In the MTS method, deviations of real models from idealized ones are observed both in magnetic and electric fields, while in the MVP method, deviations are observed only in the magnetic fields. Therefore, the MVP data are much easier to clean from distortions and obtain reliable, although not very detailed, results on the location and parameters of the electrical conductivity anomalies.

Geomagnetic field presentation. Geomagnetic variation field can be represented as a sum of three main parts: the primary external field B_{0e} of the currents in magnetosphere and ionosphere, the secondary normal internal field B_{0i} due to the currents induced in a layered 1D Earth, and the secondary anomalous field B_a . Assuming the conductivity anomaly is much smaller than the source, the anomaly-forming field can be assumed to be equal $B_0 = B_{0e} + B_{0i}$. Then the anomalous currents and fields depend linearly on the normal field strength that can be expressed by the three-dimensional tensor [Schmucker, 1970]:

$$B_a(x, y) = [b_{ik}(x, y)] B_0(x, y), \quad (1)$$

which can be expanded into

$$\begin{aligned} B_{xa} &= b_{11}B_{x0} + b_{12}B_{y0} + b_{13}B_{z0}, \\ B_{ya} &= b_{21}B_{x0} + b_{22}B_{y0} + b_{23}B_{z0}, \\ B_{za} &= b_{31}B_{x0} + b_{32}B_{y0} + b_{33}B_{z0}. \end{aligned} \quad (1')$$

The components of the magnetometer record. The sources of the fields recorded by a magnetometer can be divided into external, near-surface, and internal relative to the Earth's surface.

External fields. External fields arise from currents flow in the ionosphere and magne-

tosphere of the Earth under the influence of the solar wind, tides, and other causes.

They can be called magnetotelluric (MT) since they are used in magnetotelluric (MTS) and magnetovariational (MV) methods for studying the electrical conductivity of the Earth. Magnetosphere-ionospheric MT fields cover a range of periods from ≈ 1 second to a day; for geomagnetic deep sounding (GDS) — up to 11 years. The MT fields also include the fields of distant thunderstorms and radio stations propagating in the Earth-ionosphere waveguide which expands the range to thousands of kilohertz. Due to the high electrical conductivity of the solid Earth and oceans compared to the lower atmosphere, the MT field components behave on the Earth's surface almost like a vertically incident plane wave — the T-C model which is the theoretical basis of the conventional MTS-MVP methods. Within the framework of this model, the MT field over a horizontally layered conductivity structure has only horizontal components of the electric E and magnetic B fields (normal MT field). Over structures with a horizontally inhomogeneous distribution of electrical conductivity, the anomalous vertical and anomalous horizontal components of the magnetic field appear. As a result, the vector of geomagnetic variations tends not to the horizontal plane, as for a normal field, but to an inclined plane. Having three-component measurement data, one can determine the slope of this plane and construct the induction vector according to the ratio of the vertical component to the horizontal ones (see below the formulas 2, 3).

Near Earth's surface fields. These are mainly distortions for MT methods arising from human activities. Main sources are electrified railways, power line groundings, grounded electric motors, radio stations, cathode protection of pipelines, etc., as well as close lightning discharges and others. As a rule, they are characterized by regularities of the near wave zone [Vanyan, 1997]. For the sources listed above, the electrical components significantly prevail over the magnetic ones (compared to the MT field). If the ground source is the movement of ferromagnetic bodies (in

particular, vehicles at a short distance from the observation point), an ungrounded power line, or a line far from grounding, the magnetic components predominate.

Internal fields. Except for the electrical devices of mines and wells, all internal fields can be considered natural. The internal fields will be referred to as lithospheric emission (LE). These fields carry unique information about the earth's interior and the processes taking place there. The study of LE is at the initial stage, both in terms of the accumulation of observation data and in explaining the available observations.

Methodology. Response function (RF).

The term «Response function» in geoelectromagnetic studies carries a clear physical meaning: it is a reaction, an answer, a response of the object of the study (Earth's conductivity structure) to the action of magnetic field variations. This response carries information on the conductivity structure. Observed magnetic fields contain this response (useful information) and a great amount of excessive information about the sources of all types (MT, LE, and noise). To get rid of the excess information (about sources), we transfer data from the geomagnetic field to the response functions of the real Earth at an observation point (profile, area).

Thus, the RFs are supposed to be some functions derived from the Earth's (electro) magnetic data that allow us to facilitate the conductivity structure determination. EMRFs are usually frequency/(period T) dependent, and then they are complex functions having real (index u) and imaginary (index v) parts. The main RFs in MTS are impedance and apparent resistivity; in MVP — induction vector or tipper and horizontal magnetic tensor M . In this study we mostly use the induction vector.

Induction vector

$$C = Ae_x + Be_y, \quad (2)$$

A and B are determined from the system of linear equations:

$$B_z = AB_x + BB_y. \quad (3)$$

All three magnetic field components are composed of the normal and anomalous parts.

According to Eq. (1')

$$B_x = B_{x0} + B_{xa} = B_{x0} \left[1 + b_{11} + \left(B_{y0}/B_{x0} \right) b_{12} + \left(B_{z0}/B_{x0} \right) b_{13} \right], \quad (4)$$

$$B_y = B_{y0} + B_{ya} = B_{y0} \left[1 + b_{22} + \left(B_{x0}/B_{y0} \right) b_{21} + \left(B_{z0}/B_{y0} \right) b_{23} \right], \quad (5)$$

$$B_z = B_{z0} + B_{za} = B_{z0} (1 + b_{33}) + b_{31} B_{x0} + b_{32} B_{y0}. \quad (6)$$

Assuming $B_{z0}=0$, the solution of (3) can be presented as follows

$$A = b_{31} / \left[1 + b_{11} + \left(B_{y0}/B_{x0} \right) b_{12} \right], \quad (7)$$

$$B = b_{32} / \left[1 + b_{22} + \left(B_{x0}/B_{y0} \right) b_{21} \right]. \quad (8)$$

When using observations at one point, the normalization of the anomalous field in the vertical component is done not with respect to the anomaly-forming normal horizontal field B_0 , but to the total horizontal field (normal+anomalous). This introduces complications in the description and analysis of fields, for example, the Hilbert transform between horizontal and vertical anomalous fields along a profile is not fulfilled for the components of the induction vector. The last term in the denominators of Eqs. (7, 8) depends on the normal field's polarization, the variations of which cannot be detected by one-point observations. It can cause an error, especially large in the epicenter zone of the anomaly where the horizontal field anomaly is at its maximum (on some anomalies it approaches or exceeds 1). In the epicenter zone, the error can reach a few tens of percents, and it can manifest itself both as a data scatter and as a systematic error, which explains the unstable behavior of the induction vectors observed in nature over the anomaly axis.

Real induction vectors $C_u = A_u e_x + B_u e_y$ possess an important property: in the convention of Wiese [1965] used here, they are directed away from a good conductor, in Parkinson [1959] convention — to a good conductor.

Outline of Magnetic Variation Profiling (MVP) method. Anomalous fields of geomag-

netic variations are observed in the horizontal and vertical components, for example, over a two-dimensional body (Fig. 1). The profile curves of the horizontal anomalous field $B_{xa}(x)$ and the vertical anomalous field $B_{za}(x)$ are interconnected by the Hilbert transform, which allows the calculation of one component from the other one, thereby verifying the correctness of the anomalous field separation. The advantage of the horizontal tensor is the locality of the study: the anomalous field in the horizontal component is sensitive to the presence or absence of anomalous electrical conductivity under the observation point and its immediate surroundings, the anomalous field in the vertical component is «collected» over a large area around the observation point.

Physics of anomalous field formation. Anomalous currents in a conducting body arise due to **local electromagnetic induction inside the anomalous body**, as well as

due to **conductive redistribution** (and concentration) **of currents induced in the host medium** on a large territory comparable with the external source size. A quantitative estimate can be made based on analytical solutions for a cylinder and a sphere presented as an infinite series with the first term proportional to the applied electric field (it forms the conductive anomaly) and the second to the magnetic field (it describes the magnetic eddy type anomaly).

The solution for a cylinder (E_0 directed along the cylinder axis x) is [Svetov, 1973; Rokityansky, 1982]:

$$\begin{cases} B_{ra} \\ B_{\phi a} \\ B_{xa} \end{cases} = -\frac{1}{2} \mu_0 E_{0h} \sigma_i V \left(k_i a, \frac{\sigma_i}{\sigma_e} \right) \frac{a^2}{r} \begin{cases} 0 \\ 1 \\ 0 \end{cases} - B_{0h} D(k_i a) \frac{a^2}{r^2} \begin{cases} \sin \varphi \\ \cos \varphi \\ 0 \end{cases}, \quad (9)$$

where a — cylinder radius, σ_i and σ_e — electrical conductivity of cylinder and enclosing medium, $k^2 = -i\omega\mu_0\sigma$, $\omega = 2\pi/T$, T — period,

$$D = -\frac{I_2(k_i a)}{I_0(k_i a)} \Big|_{|k_i a| \ll 1} \rightarrow -\frac{1}{16} i\omega\mu_0\sigma_i a^2, \quad (10)$$

$$D \Big|_{|k_i a| \rightarrow \infty} \rightarrow 1$$

$$V = \frac{I_1(k_i a)}{I_0(k_i a)} \frac{2 - \frac{\sigma_e}{\sigma_i}}{k_i a} \times \frac{1 - \frac{\pi i k_i a}{2} \frac{I_1(k_i a)}{I_0(k_i a)}}{1 - \frac{\pi i k_i a}{2} \frac{I_1(k_i a)}{I_0(k_i a)}}$$

$$\times \left[\frac{I_1(k_i a)}{I_0(k_i a)} \frac{2 - \frac{\sigma_e}{\sigma_i}}{k_i a} \right] \Big|_{|k_i a| \ll 1} \rightarrow 1 - \frac{\sigma_e}{\sigma_i}, \quad (11)$$

D is a monotonically decreasing function of period, V — a monotonically increasing function of period.

Analysis of natural situations showed that the conductive-type anomalies predominate for elongated conductors, and a corresponding theory was developed for them [Roki-

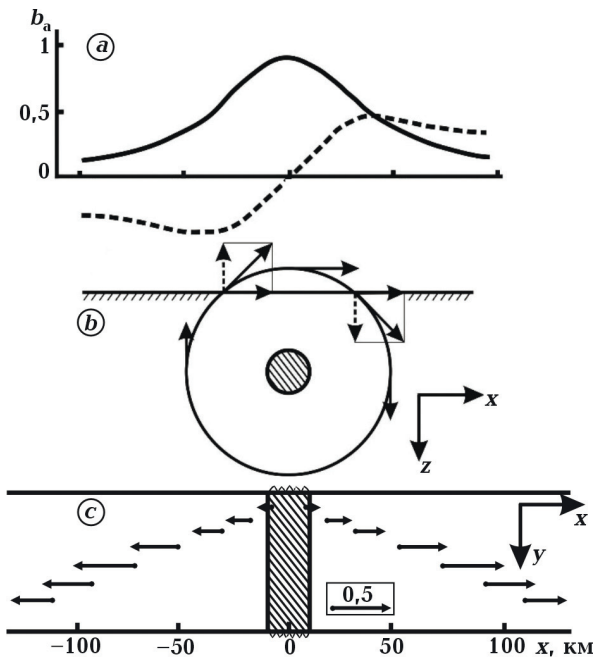


Fig. 1. Formation of horizontal H_{xa} (solid curve) and vertical H_{za} (dotted curve) projections of anomalous magnetic fields over a two-dimensional conductor: *a* — profile plots of the anomalous field normalized to the normal field; *b* — an anomalously conducting cylinder and the line of force of the anomalous magnetic field around it, decomposed into horizontal and vertical components; *c* — real induction vector at a profile crossing a 2D anomaly. The model parameters roughly correspond to the Kirovograd anomaly.

tyansky 1975, 1982, p. 247—277, 290—307]. The frequency characteristics of the conductive-type anomalous field are equal to the product of two functions. The first one is the non-decreasing function $V(T)$ ($0 \leq V \leq 1$, $V=1$ corresponds to DC (Fig. 2)) which describes the degree of filling of the conductor by anomalous currents (result of the skin effect inside the anomalous body with conductivity σ_i). The other function is the normal imped-

ance (decreasing function of period T (Fig. 3)) *a priori* studied by the GDS-MTS soundings.

The normal impedance is a decreasing function of the period, so its product with function V has a maximum at some period T_0 (Fig. 4, 5). The position T_0 is closely related to the total longitudinal conductance $G[S \times m]$ of the anomalous body, that is, the scale of the anomaly. On the period T_0 , the anomalous fields and the induction vector be-

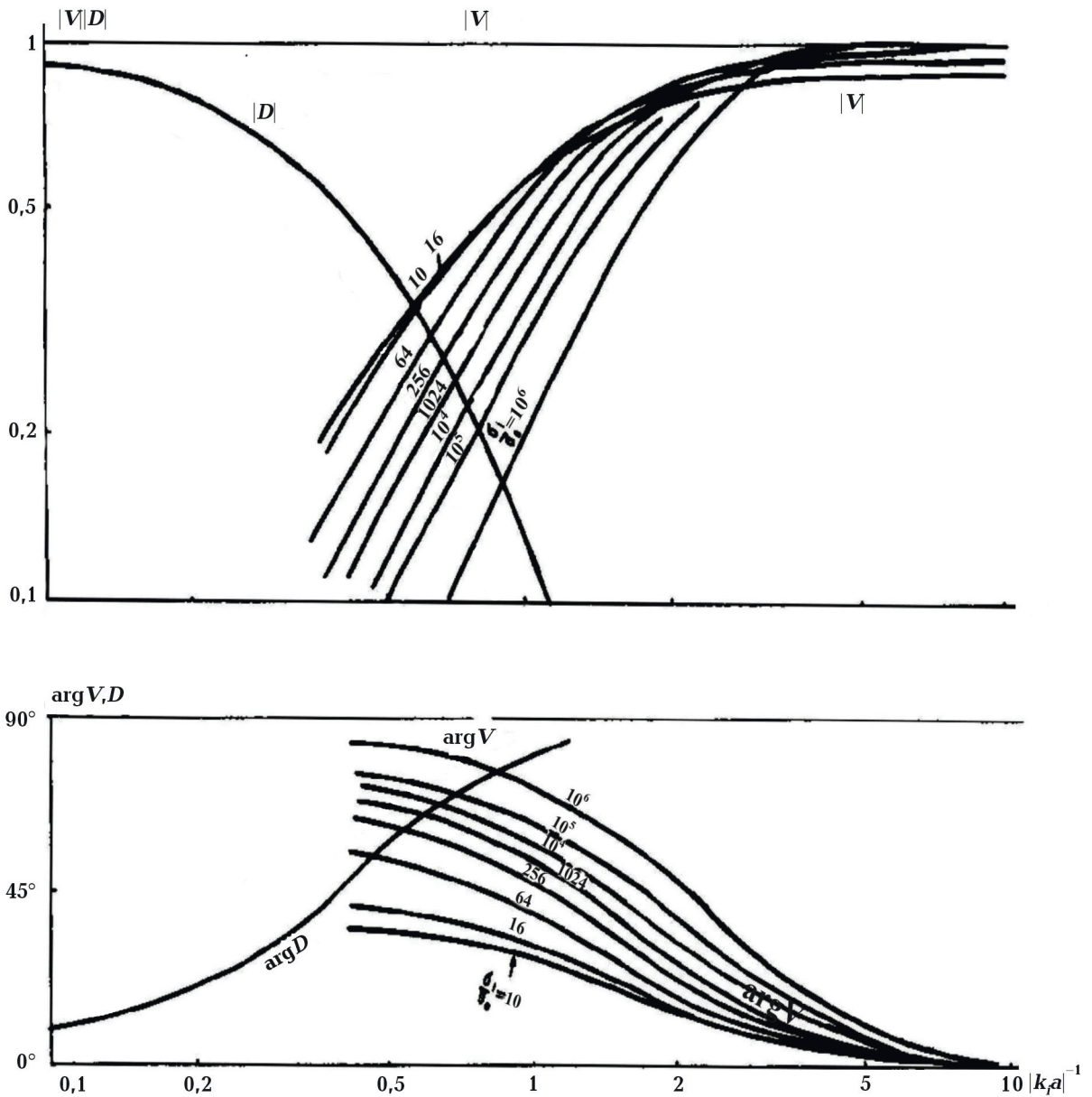


Fig. 2. Functions V and D for a circular cylinder with different σ_i/σ_e (curve index) along the horizontal axis $[k'a]^{-1}$ proportional to T . Phase sign is for time factor $\exp(+i\omega t)$.

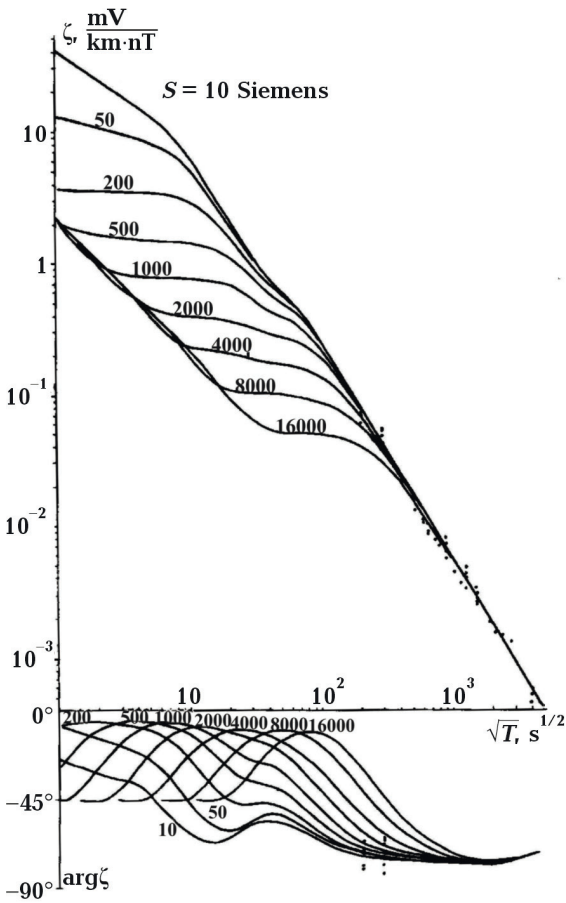


Fig. 3. Normal impedance from the global GDS observations (given by dots) with calculated effect for a cross-section containing asthenosphere ($h=100$ km, $S=1000$ S) and surface conducting layer of conductance given in Siemens (curve index). Phase sign is for $\exp(+i\omega t)$.

come real $C=C_u$ and the imaginary induction vector C_v passes through zero changing sign. On shorter periods, C_u and C_v are parallel, on longer periods they are anti-parallel for a 2D anomaly. These relations are valid for time factor $\exp(+i\omega t)$. For $\exp(+i\omega t)$ they are *vice versa*.

Consider Fig. 4. Models A, B and E are the surface conductors with $a/b=1/16$. The smallest anomalous body A has $G=10^3$ S·m and

Model	$G, S\cdot m$	T_0, s	h, km
A	10^3	0.004	0
B	10^5	0.4	0
C	$0.625\cdot 10^6$	3.5	1.05
D	$0.625\cdot 10^8$	350	10.5
E	10^9	4000	0

$T_0=0.004$ s. The largest, E, has $G=10^9$ S·m and $T_0=4000$ s. Direct proportionality between G and T_0 is clearly seen: $G[S\cdot m]=T_0[s]\cdot 25\cdot 10^4$.

Models C and D are vertical bodies with $a/b=4/1$ immersed at depth h . The direct proportionality between G and T_0 keeps but with another coefficient which differs from the A, B and E models coefficient by $\approx 28\%$: $G[S\cdot m]=T_0[s]\cdot 17.86\cdot 10^4$.

Wide-surface models A-B-E are almost opposite to narrow deep models C-D. Thus, it can be assumed that 2D models of different shapes and depths have an intermediate coefficient of proportionality between the two types of models considered, namely $G[S\cdot m]=T_0[s]\cdot (21\pm 4)\cdot 10^4$.

The models in Fig. 4 are calculated for a homogeneous half-space. In the real Earth, the conductivity globally increases with depth, extensive conductive layers can exist in shallow strata (asthenosphere, surface layers of sediments or water) forming a variety of normal impedances, as presented in Fig. 3. The impedance of homogeneous half-space is described by straight line declined at an angle of 45 degrees. Impedance of the real Earth measured by global Geomagnetic Deep Sounding for period interval of 1 day — 11 years declined at ≈ 53 degrees (see Fig. 3), hence the dependence of G on T_0 will be non-linear. Known anomalies have T_0 in the range of 500—4000 s. At these periods, normal impedance depends on the conductance of asthenosphere and near-surface layers, and between G and T_0 various relations can arise.

In the book [Rokityansky, 1982], the anomalous fields of various conducting models available at that time were analyzed and an empirical formula was obtained [Rokityansky, 1982, p. 295, Table 23, line IV]

$$G[S\cdot m]=5\cdot 10^4\cdot (T_0[s])^{1.2}, \quad (12)$$

which was used in practice.

Short specification of the MVP method. A necessary and sufficient condition to draw the conclusion about the existence of an electrical conductivity anomaly is the existence of a geomagnetic variation's anomaly.

The existence of an anomaly of geomagnetic variations is evident from the stable

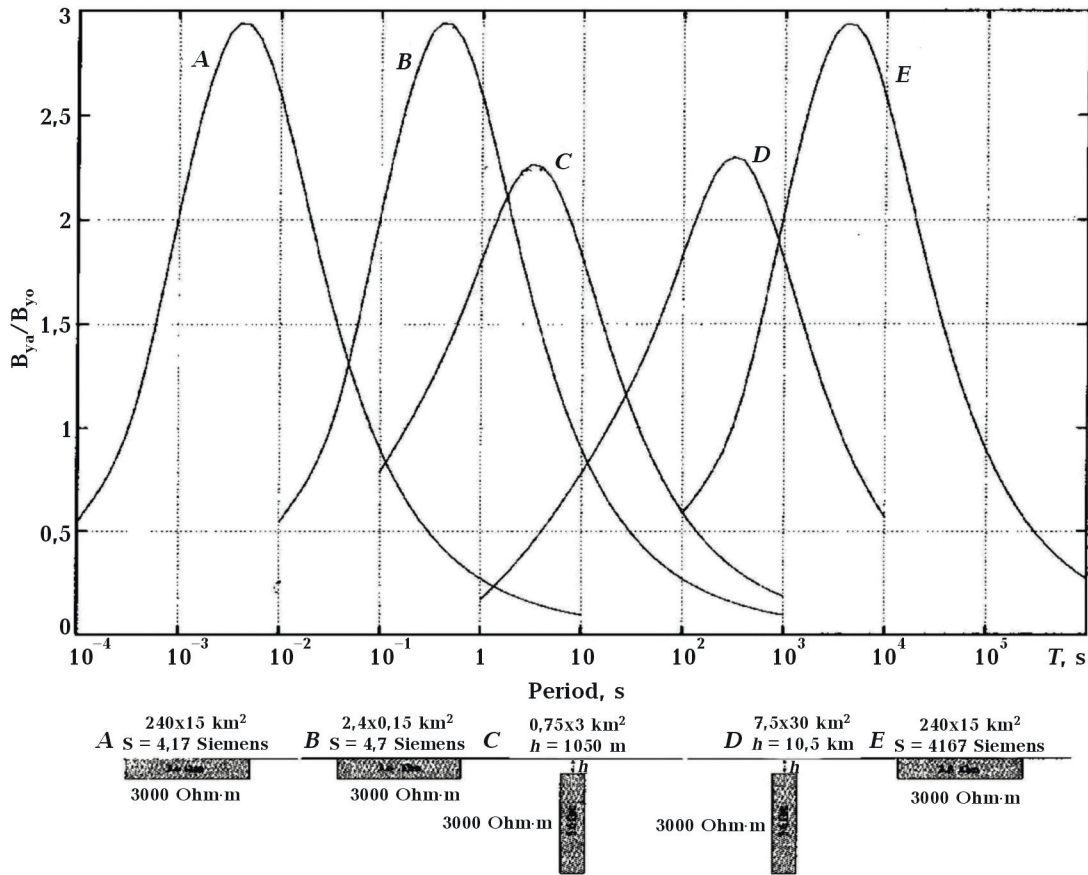


Fig. 4. Frequency characteristic of the horizontal component of the anomalous field over the anomalous body with specific resistivity $\rho_f=3.6$ Ohm·m embedded in uniform half-space $\rho_e=3000$ Ohm·m, the anomalous body has a rectangular cross-section $a \times b$ with a different size and total lengthwise conductance $G=a \times b / \rho_f$ forming 5 variants with parameters presented in the Table.

presence of vertical component and from the difference in horizontal components at moderately spaced sites.

The shape of the profile curves of the anomalous field yields reliable estimation of the maximum possible depth of the anomalous currents' center d and the width $2L$ of the anomaly.

The frequency response of the anomalous field yields an estimate of the total lengthwise conductance G of the long (2D) anomalous body.

The simple completely reliable MVP pre-computer results (anomaly location, d , L and G with their uncertainties) should be used as *a priori* information for subsequent thorough MVP-MTS inverse problem computer modeling.

MTS impact. MVP data are poorly sensi-

tive to the depth of the upper edge h of the anomalously conducting body. This depth should be determined by sounding methods, primarily by MTS, which can be challenging. For example, 25 MTS soundings were specially performed to determine h — the depth of the upper edge of the Kirovograd anomaly (KirA). On the Ukrainian Shield (USh) and Dnieper-Donets basin, h was determined with a large scatter due to distortions from near-surface heterogeneities, which did not allow drawing a conclusion about spatial changes in h , and only an average of 15 MTS curves result $h=15 \pm 5$ km was obtained [Rokityansky et al., 2012]. The remaining 10 MTS were placed on the southern slope of the USh, on the South Ukrainian monocline along the profile above the KirA axis. These MTS curves had long ascending branches and did not «sense» the

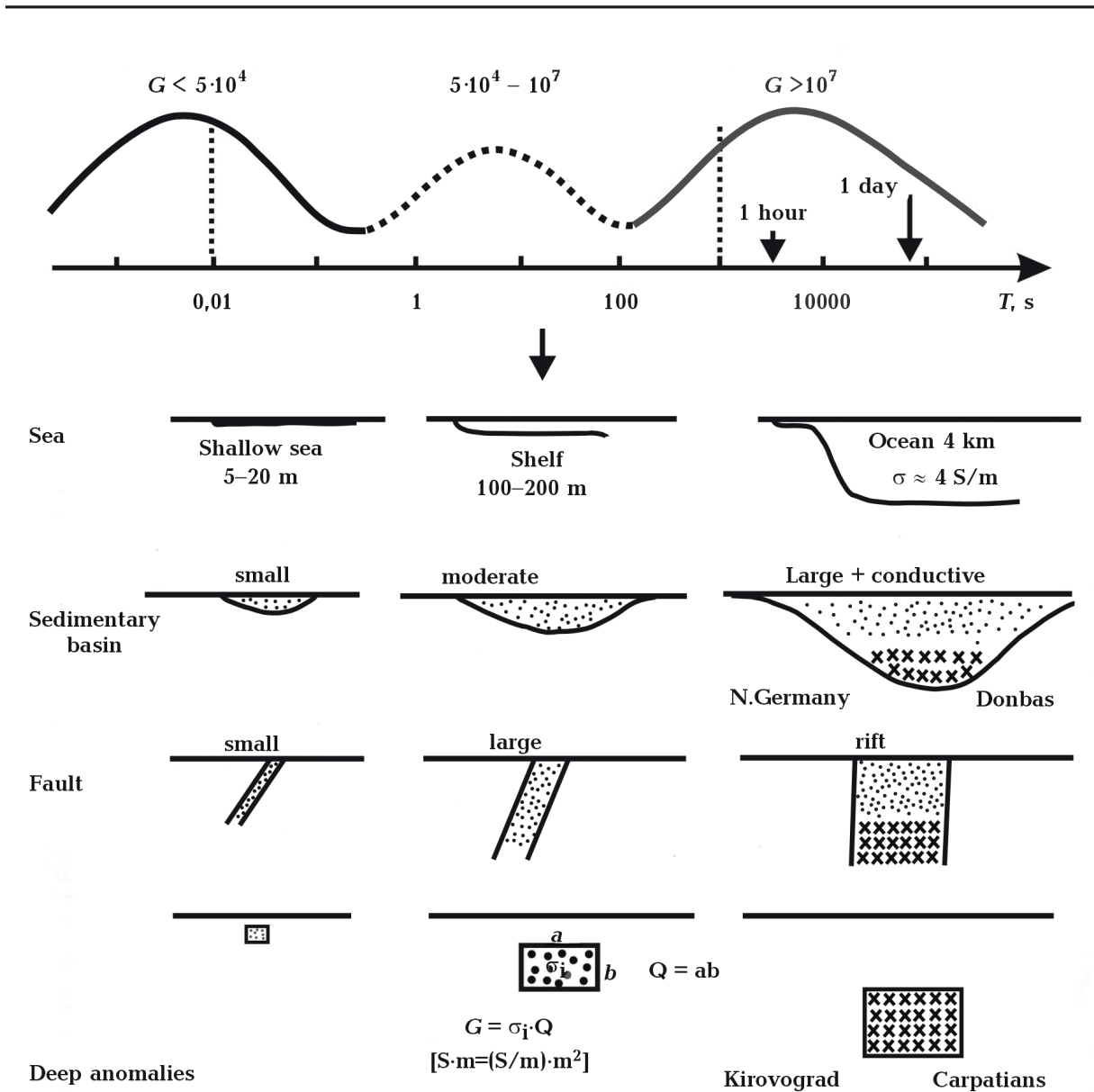


Fig. 5. Examples of conductivity anomalies and the relation of their conductance G with the position of frequency response maximum T_0 .

presence of the KirA anomaly, clearly visible from the MVP data. The reason is shielding by sloping layers of sedimentary rocks [Berdichevsky, Dmitriev, 2008]. Conclusion: MTS should be carried out in conjunction with the MVP, with the latter having priority.

Having both vectors at one (or at short band) period, it is possible to determine from their ratio sign where the T_0 period is located and obtain a one-side estimate of G . This is true for two-dimensional anomalies. The non-parallelism of C_u and C_v is a feature of the

three-dimensionality of the geoelectric structure but this does not necessarily mean the absence of a 2D anomaly which can extend through/inside/beside some wider or separate anomalous structure. Induction vectors C_u and C_v along some known quasi-2D elongated anomalies (e.g., Carpathian or Kirovograd ones) in some places are not parallel. At that C_u is naturally directed from the anomaly axis; however, C_v can randomly decline from C_u 's direction in some places by action of some local or intersecting conducting structure(s).

Elongated anomalies with varying cross section.

Below we will briefly consider two opposite cases — an elongated anomaly narrows or expands away from the observation profile/area (Fig. 6). T_0 describes the effects of the finite length of the anomaly; the results of computer calculations [Weidelt, 1975] and physical modeling [Rokityansky, 1975] are used. Of the many results obtained, we present a graph of calculations of the anomalous field over a conducting spheroid with different elongation l/a (Fig. 7). The model's parameters are typical for real geoelectric conditions. With these parameters, the observed maximum of the frequency response $T_0=500\div 4000$ s is realized at spheroid elongations of 40—60. Perhaps such elongations are typical in nature. For the description of anomaly widening, the results of physical modeling [Rokityansky, 1975, 1989] are used. Area of measurements and study is located between the wider or more conductive parts of the anomaly (Fig. 6, c). A similar situation is observed in sea straits which is why this phenomenon is called the strait effect. Its characteristic feature is an increase in electric and magnetic fields compared with the 2D case, while in case A (Fig. 6, a) it is *vice versa* — a decrease in both fields.

In the book [Rokityansky, 1982, p. 302—305], a method for determining G from MTS data was described and the following conclu-

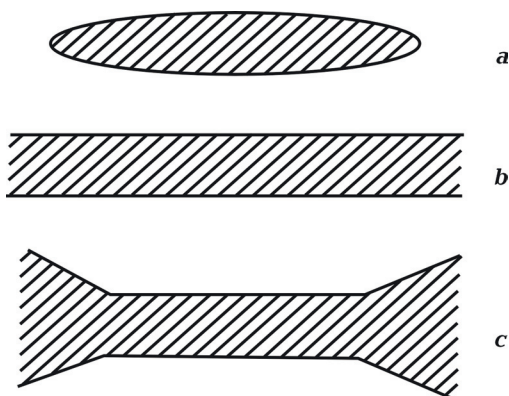


Fig. 6. Three models of cross-section variations: a — narrowing cross-section including finite-length anomalies creates body-end effect and shunt effect in MTS data; b — 2D anomalies; c — expanding cross-section creates the strait effect or super-channeling effect.

sions were substantiated:

If $G_{MVP} < G_{MTS}$, then G of the anomaly outside observation area decreases («shunt effect» or «body-end effect»),

If $G_{MVP} > G_{MTS}$, then G of the anomaly outside observation area increases («strait effect» or «super-channeling effect»).

Some results of MVP studies. Many electrical conductivity anomalies have been found and studied using induction vectors and anomalous fields in horizontal magnetic components.

Large anomalies in Eastern Europe:

Kirovograd (1969), $G=2\cdot 10^8$ S·m [Rokityansky et al., 2012, 2018],

Carpathian (1972), $G=2\cdot 10^8$ S·m,

Moscow—Tambov (1977), $G=2\cdot 10^8$ S·m,

Ladoga (1981), $G=2\cdot 10^8$ S·m. MTS was carried out there before the MVP but the anomaly was discovered with MVP data [Rokityansky et al., 2018].

Donbas (1988), $G=8\cdot 10^8$ S·m. In the data of more than twenty MTS and records of pulses from the Volgograd-Donbas long (487 km) line, the anomaly cannot be clearly distinguished.

Other regions large-scale anomalies:

Andean (Peru, Bolivia, Chile) $G=8\cdot 10^8$ S·m,

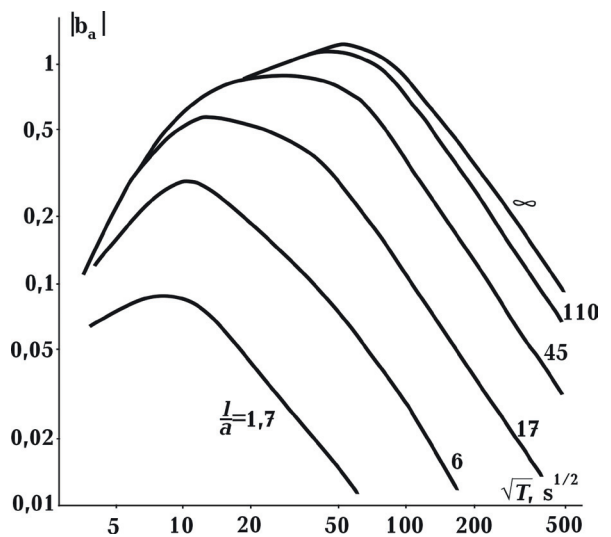


Fig. 7. Horizontal anomalous field over a conducting spheroid with different elongation l/a (curve index). Spheroid of radius $a=20$ km and conductivity $\sigma_i=1$ S/m is embedded at depth $h=20$ km in a 100-km thick layer of resistivity $\rho_e=10^3$ Ohm·m. Below 100 km, normal cross-section obtained by GDS sounding. l — spheroid length.

North Germany $G=8\cdot 10^8$ S·m,
 Verkhoyansk (NE Siberia) $G=4\cdot 10^8$ S·m,
 Igdlorssuit in Western Greenland
 $G=3.5\cdot 10^8$ S·m,
 Three long anomalies in Western North
 America $G=3\cdot 10^8$ S·m,
 Adelaide in Southern Australia $G=3\cdot 10^8$ S·m,
 Alert in Northern Canada $G=2\cdot 10^8$ S·m,
 South-West African $G=2\cdot 10^8$ S·m,
 Caucasian, Ural, Transdanubian
 $G\approx 1\cdot 10^8$ S·m.

These G determinations were made based on the single dependence of G on T_0 according to the empirical formula 12 without considering the anomaly's form and depth and changes in the normal impedance in each region. This lack of accounting can yield an uncertainty of up to a few dozen %. Nevertheless, these data reliably show that the scale of the crustal conductivity anomalies is not uniformly distributed; namely, **the maximum number of anomalies have G in a relatively narrow range of $(1-8)\cdot 10^8$ S·m.** This result has geophysical significance. It is natural. Many natural objects have characteristic sizes: rifts, sedimentary basins, depths (and widths) of near-coastal shallows, shelves, oceanic plates, oceanic subduction troughs etc. (see Fig. 5).

We believe that measurement and calculation of T_0 and G parameters would be very useful characteristics of every anomaly. These parameters can be different in various profile sites, for horizontal (tensor M) and vertical (tipper) components, in different parts of the anomaly. These facts are also interesting for study. Their analysis requires an understanding of their formation's physics that can help to get a new insight into the geoelectrical structure.

In Fig. 4, 5, maxima of the anomalous field are given for separate conductors. If the scales G of two anomalies differ by two or more orders, then their frequency characteristics can be seen as separated maxima (as in Fig. 4) in the record of one well-located observatory. One example of such anomalies is the shelf 100—200 m deep and the deep ocean ≈ 4 km deep. Such an example can be seen in the work by Rigaud et al. [2021] on two islands in the Indian Ocean: at observatory CKI (In-

termagnet code), the northern component of the induction vector has two maxima with $T_0=15$ and 1500 s, at observatory GAN, the eastern component has maxima at periods 20 and 4000 s.

The existence of maxima of the anomalous field reveals its quasi-resonance properties, an important manifestation of which is the change of sign of the imaginary part of the anomalous field. Such a tendency to change the sign of the imaginary part of the dominant Q -response against the background of an increase in the real part in the period interval from 200 to 2 days was observed and described in [Kuvshinov et al., 2021, Fig. 8]. We can suppose that resonance period T_0 is located somewhere at shorter period, let us say at period one day. This RF resonance can be a manifestation of the EM field (quasi-) oscillations on the global electrical conductivity structure penetrated by the EM field described by the dominant Q -response [Kuvshinov et al., 2021]. This global EM quasi-oscillation may be considered as an analog of the true mechanical oscillations of the Earth.

Conclusions. The method of magnetic variation profiling (MVP) with its main tools being the induction vector and the horizontal tensor yields reliable results on the existence and location of an anomaly, gives an estimate of its maximum possible depth and width, as well as, under some assumptions, an estimate of its integral conductance G .

1. These MVP parameters, obtained immediately after the processing of the geomagnetic field, should be used as reliable *a priori* information in the further detailed computer solution of the inverse problem.

2. The spectral properties of the geomagnetic response functions were studied for two-dimensional anomalies with a generalization to three-dimensional conductors with varying cross-section — cases of the anomaly narrowing or widening outside of the observation area.

3. 18 crustal electrical conductivity anomalies were considered and their integral lengthwise conductance G was obtained. At all anomalies, G values turn out to be in a relatively narrow range $G=(1-8)\cdot 10^8$ S·m.

This result has geophysical significance.

4. The rotational movements in which the Earth participates (or in the field in which it is located) are characterized by a set of periodicities. The main ones are the day, month, year, solar cycles, planetary configurations and others. The study of these periodicities in

various phenomena (including geomagnetic variations) can provide new information and understanding. Variations of the induction vector are characterized by local and non-local features, decoding of which can provide an additional information channel, both from the bowels of the Earth and from space.

References

- Berdichevsky, M.N., & Dmytriev, V.I. (2008). *Models and methods of magnetotellurics*. Berlin-Heidelberg: Springer Verlag, 679 p.
- Kuvshinov, A., Grayver, A., Töfner-Clausen, L., & Olsen, N. (2021). Probing 3-D electrical conductivity of the mantle using 6 years of Swarm, CryoSat-2 and observatory magnetic data and exploiting matrix Q-responses approach. *Earth, Planets and Space*, 73, 67. <https://doi.org/10.1186/s40623-020-01341-9>.
- Parkinson, W.D. (1959). Direction of rapid geomagnetic fluctuations. *Geophysical Journal of Royal Astronomical Society*, 2(1), 1—14. <https://doi.org/10.1111/j.1365-246X.1959.tb05776.x>.
- Rigaud, R., Kruglyakov, M., Kuvshinov, A., Pinheiro, K., Petereit, J., Matzka, J., & Marshalko, E. (2021). Exploring effects in tippers at island geomagnetic observatories due to realistic depth- and time-varying oceanic electrical conductivity, *Earth, Planets and Space*, 73, 3. <https://doi.org/10.1186/s40623-020-01339-3>.
- Rokityansky, I.I. (1975). *Investigation of electrical conductivity anomalies by magnetovariational profiling method*. Kiev: Naukova Dumka, 279 p. (in Russian).
- Rokityansky, I.I. (1982). *Geoelectromagnetic investigation of the Earth's crust and upper mantle*. Berlin-Heidelberg-New York: Springer Verlag.
- Rokityansky, I.I. (1989). Modeling of 3D-effects on electrical conductivity anomalies. *Geofizicheskiy Zhurnal*, 11(4), 28—36 (in Russian).
- Rokityansky, I.I., Tereshyn, A.V., Tregubenko, V.I., Golubtsova, N.S., Ingerov, A.I., & Savchenko, T.S. (2012). Review of MVP-MTS observations in the southern part of the Kirovograd electrical conductivity anomaly and the first experience of film modeling of the structure of the Ukrainian shield. *Geofizicheskiy Zhurnal*, 34(3), 92—101. <https://doi.org/10.24028/gzh.0203-3100.v34i3.2012.116644> (in Russian).
- Rokityansky, I.I., Sokolova, E.Yu., Tereshyn, A.V., Yakovlev, A.G., & LADOGA Working group. (2018). Electrical conductivity anomalies in the joint zones of Archean and Proterozoic geoblocks on the Ukrainian and Baltic Shields. *Geofizicheskiy Zhurnal*, 40(5), 208—244. <http://dx.doi.org/10.24028/gzh.0203-3100.v40i5.2018.147490> (in Russian).
- Schmucker, U. (1970). *Anomalies of geomagnetic variations in the southwestern United States*. Bull. Scripps Inst. Oceanogr. 13, 165 p.
- Svetov, B.S. (1973). *Theory, methods and interpretation of the low frequency inductive electrical prospecting data*. Moscow: Nedra, 254 p. (in Russian).
- Vanyan, L.L. (1997). *Electromagnetic soundings*. Moscow: Nauchnyy Mir, 218 p. (in Russian).
- Weidelt, P. (1975). Electromagnetic induction in three-dimensional structures. *Journals of Geophysics*, 41, 85—109.
- Wiese, H. (1965). *Geomagnetische Tiefentelluric*. Berlin: Akad. Verlag, 146 p.

Дослідження аномалій електропровідності

І.І. Рокитянський, А.В. Терешин, 2023

Інститут геофізики ім. С.І. Субботіна НАН України, Київ, Україна

Аномальні струми в добре провідних тілах виникають унаслідок локальної електромагнітної індукції всередині аномальних тіл, а також кондуктивного перерозподілу (і концентрації) струмів, індукованих у вмістному середовищі, на великій території, що порівнянна з розміром зовнішнього джерела. Локальна індукція породжує так звану аномалію геомагнітних варіацій магнітного типу. Її характерна властивість — вторинне аномальне поле не може бути більшим за первинне нормальне поле геомагнітних варіацій. Втім у деяких місцях на земній поверхні аномальні поля (нормовані) перевищують одиницю. Аналітичний розв'язок задачі електромагнітної індукції для круглого циліндра дає фізичне пояснення двох типів аномальних геомагнітних полів. Перший член (пропорційний нормальному електричному полю E_0) описує провідний тип аномалії, другий член (пропорційний нормальному магнітному полю B_0) — індукційний тип аномалії. Перший тип зазвичай набагато більший, ніж другий. Аномальні поля провідного перерозподілу не обмежуються одиницею чи будь-яким іншим числом. Вони пропорційні двом функціям: $V(T)$ — неспадна функція періоду T ($0 \leq V \leq 1$, $V=1$ відповідає постійному струму), яка описує ступінь заповнення провідника аномальними струмами (результат скін-ефекту всередині аномалії); і нормальний імпеданс навколишнього середовища — спадна функція періоду. Добуток таких функцій має максимум на деякому періоді T_0 , положення якого тісно пов'язане із повною поздовжньою провідністю G [$S \times m$] — аномального тіла, тобто масштабом аномалії. На періоді T_0 аномальні поля і вектор індукції стають дійсними $C=C_u$, уявний вектор індукції C_v проходить через нуль зі зміною знака. Отже, спектральні властивості геомагнітних функцій відгуку були вивчені для двовимірних аномалій з узагальненням на тривимірні провідники зі змінним поперечним перерізом. Розглянуто 18 аномалій електропровідності земної кори та отримано їх інтегральну поздовжню провідність G . Для всіх аномалій значення G лежать у відносно вузькому діапазоні $G=(1-8) \cdot 10^8$ См·м, що має геофізичне значення.

Ключові слова: електричні властивості, електромагнітна теорія, геомагнітна індукція, вектор індукції, магнітоваріаційне профілювання.